

# A Mathematics Approach to Improve the Computational Efficiency of Economic-oriented Model Predictive Control

Yizhou Fang and Antonios Armaou

**Abstract**—In this paper, we propose a mathematics approach to improve the computational efficiency of economic-oriented model predictive control (EMPC). We approximate the nonlinear dynamic system with a Two-tier method: 1) Approximate the system through Taylor expansion and obtain a polynomial formulation; 2) Expand the polynomial formulation through Carleman approximation (also known as Carleman linearization) and arrive at an extended bilinear expression. This expression has a bilinear form but carries information of higher order dynamics. In this way, we save simulation efforts by predicting the future economic performances with analytical solutions. We also save optimization efforts by providing the sensitivity of the economic performances to the manipulated inputs as the search gradient. Hence, despite the economic stage costs are mostly non-tracking and non-quadratic, we achieve significant acceleration in the computation of EMPC. An oxidation of ethylene reactor is demonstrated as the application example. We optimize three manipulated inputs and establish a non-tracking cyclic operation. The improvement in computational efficiency is presented by comparison with standard EMPC method.

## I. INTRODUCTION

In recent years, economic-oriented model predictive control (EMPC) has gained popularity in chemical and petrochemical industries. The primary difference of EMPC from traditional MPC is that EMPC is directly formulated to maximize the economic profits. It naturally puts more emphasis on the process path [1][2]. Typically, the economic operation of a process is a two-layer scheme [3]. The upper layer is the real-time optimization (RTO) layer, which performs economic process optimization and determines the optimal operation trajectory. The lower layer is the MPC layer. It forces the system to track the optimal process trajectory obtained from the upper layer and to reject disturbances. However, the RTO results may be inconsistent with the MPC objectives and may lead to infeasibility. These issues give rise to the development of EMPC.

An increasing number of results on EMPC studies was recently published; [4] presents a good review. However, one of the remaining major challenges is the heavy burden on computation. Unlike traditional tracking MPC, the economically optimal cost functions representing the economic performances, are usually non-quadratic or even non-convex.

Yizhou Fang is with the Department of Chemical Engineering, the Pennsylvania State University, University Park, PA 16802. Antonios Armaou is with the Department of Chemical Engineering, the Pennsylvania State University, University Park, PA 16802 and Department of Mechanical and Electrical Engineering, Wenzhou University. Corresponding author, email: armaou@enr.psu.edu

Financial support from the National Science Foundation, CBET Award 12-64902 is gratefully acknowledged.

They may require significant amount of simulation and put heavy load of work on the optimizer. If the optimizer fails to converge to the solution fast enough, the delay in sending the control signals, or sending non-converged control signals may degrade its closed loop performance, or even cause potential stability issues. There are formulations to guarantee the stability of systems under EMPC, including adding quadratic regularization terms in the economic cost function, applying terminal constraints, and using Lyapunov-based constraints [5][6]. These formulations further exacerbate the computational burden of EMPC.

There have been approaches reported in literature to achieve computational acceleration. For example, multi-parametric MPC developed by Pistikopoulos and coworkers in [14][15] accelerates computation via querying response hypersurfaces. Fast approaches to solve for MPC have also been reported in applications, such as lithium-ion battery systems [16][17][18]. To address the computational issue of EMPC, we propose an approach based on Carleman approximation. It builds on our previous work that focused on efficient reformulations of nonlinear MPC (NMPC) published in [7][8][9][10]. Carleman approximation-based Moving Horizon Estimation (MHE) methods are reported in [11][12]. In this paper, we intend to show the readers the readiness of our approach when working with non-tracking economic stage costs and path-emphasized optimization. Our approach significantly reduces computational efforts in EMPC context.

The approach we are proposing is built upon two foundations: the theory of Carleman approximation and the theory of bilinear control systems. After a Two-Tier approximation, we use high order polynomial states to capture the nonlinearity of the original dynamic process. With an extended bilinear expression and assuming piecewise constant manipulated inputs, we analytically predict future states and future economic performances. We also analytically calculate the sensitivity of the economic cost function to the manipulated inputs. The sensitivity serves as the gradient to facilitate the optimizer by reducing the number of iterations tremendously. Hence, the computational effort in solving the EMPC problem is sufficiently reduced. This approach circumvents feedback delays in the following two ways: First, the economic performance of the plant becomes a nonlinear function of the manipulated inputs, releasing the optimization problem from equality dynamic constraints. Second, it analytically predicts future economic performance of the system and provides the sensitivity as the search gradient to facilitate the optimizer.

## II. DEFINITION AND FORMULATION

### A. Basic EMPC formulation

The plant, which is a continuous system, is represented by the following ordinary differential equation (ODE):

$$\begin{aligned} \dot{x} &= f(x) + \sum_{j=1}^m g_j(x)u_j(t) \\ x(t_0) &= x_0 \end{aligned} \quad (1)$$

$f(x)$  and  $g_j(x)$ ,  $j = 1, \dots, m$  are nonlinear vector functions.  $u_j(t)$  denotes the  $j$ -th design variable vector.  $x_0$  denotes the initial system states at the starting time  $t_0$ .

The stage cost, representing the process economics over each sampling time, is expressed as:

$$\begin{aligned} \int_{t_{i-1}}^{t_i} L_e(x(\tau), u_1(\tau), u_2(\tau), \dots, u_m(\tau))d\tau, \\ \forall i = 1, \dots, N \end{aligned} \quad (2)$$

In this context, the overall economic cost function, which describes the economic performance of the plant, is maximized over a finite time window, the prediction horizon.

$$\begin{aligned} \int_{t_0}^{t_N} J_e(x(\tau), u_1(\tau), u_2(\tau), \dots, u_m(\tau))d\tau \\ = \sum_{i=1}^N \int_{t_{i-1}}^{t_i} L_e(x(\tau), u_1(\tau), u_2(\tau), \dots, u_m(\tau))d\tau \end{aligned} \quad (3)$$

$t_0$  and  $t_N$  denote the starting and ending of the prediction horizon.

The economically optimal control problems are recast as receding finite horizon dynamic optimization ones. We use control vector parameterization (CVP) to reformulate dynamic optimization problems (DOP) as finite dimensional nonlinear programming (NLP) ones [13]. The basic principle is to express the manipulated inputs in a finite vector of design variables as the parameters to be optimized [19][20]. Assuming piecewise constant manipulated inputs during every sampling time, the EMPC problem has a general form:

$$\begin{aligned} \max_{u_1, u_2, \dots, u_m, t_0} \int_{t_0}^{t_N} J_e(x, u_1(\tau), u_2(\tau), \dots, u_m(\tau))dt \\ \text{s.t.} \\ u_j(t) = \sum_{i=1}^N u_{j,i} \mathbf{B}(t; T_{i-1}; T_i), \\ \forall j = 1, \dots, m \\ \dot{x} = f(x) + \sum_{j=1}^m g_j(x)u_j(t) \\ x(t_0) = x_0 \\ x_{min} \leq x(t) \leq x_{max}, \forall t \in [t_0, t_N] \\ u_{min} \leq u(t) \leq u_{max}, \forall t \in [t_0, t_N] \\ f^c(x, u_1, u_2, \dots, u_m) \leq 0 \end{aligned} \quad (4)$$

$x \in R^n$  is the vector of states, and  $u_j$ ,  $j = 1, \dots, m$  are the vectors of the manipulated inputs, which are the design variables.  $u_{j,i}$  denotes the  $i$ -th element in the  $j$ -th design variable vector. We use  $u$  to represent all of them in the rest of this manuscript. From a view of control, it denotes the

$i$ -th signal of the  $j$ -th manipulated input in its corresponding time period  $(T_{i-1}, T_i]$ . The time period  $(T_{i-1}, T_i]$  is defined as the  $i$ -th sampling time and has a length of  $\Delta T_i = T_i - T_{i-1}$ . We define a pulse function with  $\mathbf{B}(t; T_{i-1}; T_i) = \mathbf{H}(t - T_{i-1}) - \mathbf{H}(t - T_i)$ , where  $\mathbf{H}$  is the standard Heaviside function.  $N$  is the total number of the sampling times within each control horizon.  $T_0$  and  $T_N$  are the beginning and the end of the control horizon, respectively. In typical MPC designs, the length of the prediction horizon is usually greater than the control horizon, depending on the robustness requirement. In this paper, we set the prediction horizon equal to the control horizon for the purpose of simplicity. The last three equations denote the bounds on the states, on the manipulated inputs, and any other equality/inequality constraints on the system. These constraints may account for physical limitations, safety concerns, and other requirements on the system performance.

### B. Two-Tier approximation

#### Tier One

For the simplicity of derivation, we perform Taylor expansion around the origin  $x = 0$ . In NMPC problems, the desired steady states, which we try to track, are often the ideal points to perform Taylor expansion around. In EMPC problems, unlike traditional MPC, there are usually not any desired steady states to track. In these cases, we pick the steady states within or close enough to the economically optimal set to perform Taylor expansion around.

Nonlinear vector functions  $f(x)$  and  $g_j(x)$  are expanded by Maclaurin series in the following form:

$$f(x) = f(0) + \sum_{k=1}^{\infty} \frac{1}{k!} \partial f_{[k]}|_{x=0} x^{[k]} \quad (5)$$

$$g_j(x) = g_j(0) + \sum_{k=1}^{\infty} \frac{1}{k!} \partial g_{j[k]}|_{x=0} x^{[k]} \quad (6)$$

$x^{[k]}$  denotes the  $k$ -th order Kronecker product of  $x$ . Details of the Kronecker product rule are presented in the next section.

$\partial f_{[k]}|_{x=0} \in C^{n \times (n^k)}$  and  $\partial g_{j[k]}|_{x=0} \in C^{n \times (n^k)}$  are the  $k$ -th partial derivatives of  $f(x)$  and  $g_j(x)$  with respect to  $x$ , based on the Kronecker product rule:

$$\partial f_{[k]} = \frac{\partial}{\partial x} \otimes \partial f_{[k-1]}, \quad \partial g_{j[k]} = \frac{\partial}{\partial x} \otimes \partial g_{j[k-1]}, \quad (7)$$

For example, if  $x = [x_1 \ x_2]$ ,  $k = 2$ ,

$$\partial f_{[2]} = \begin{bmatrix} \frac{\partial^2 f}{\partial x_1^2} & \frac{\partial^2 f}{\partial x_1 \partial x_2} & \frac{\partial^2 f}{\partial x_1 \partial x_2} & \frac{\partial^2 f}{\partial x_2^2} \end{bmatrix} \quad (8)$$

With the approximations above, the nonlinear dynamic system described by Eq. (1) can be approximated with the following polynomial form:

$$\begin{aligned} \dot{x} &\cong \sum_{k=1}^p A_k x^{[k]} + A_0 + \sum_{j=1}^m \left( \sum_{k=1}^p B_{jk} x^{[k]} + B_{j0} \right) u_j \\ A_k &= \frac{1}{k!} \partial f_{[k]}|_{x=0}; \quad B_{jk} = \frac{1}{k!} \partial g_{j[k]}|_{x=0}; \\ A_0 &= f(0); \quad B_{j0} = g_j(0); \end{aligned} \quad (9)$$

### Tier Two

We now introduce the Kronecker product rule to facilitate the description of Carleman approximation. The Kronecker product of matrix  $X \in C^{N \times M}$  and matrix  $Y \in C^{L \times K}$  is defined as matrix  $Z \in C^{(NL) \times (MK)}$ .

$$X = \begin{bmatrix} x_{1,1} & x_{1,2} & \cdots & x_{1,M} \\ x_{2,1} & x_{2,2} & \cdots & x_{2,M} \\ \cdots & \cdots & \cdots & \cdots \\ x_{N,1} & x_{N,2} & \cdots & x_{N,M} \end{bmatrix}, Y = \begin{bmatrix} y_{1,1} & y_{1,2} & \cdots & y_{1,K} \\ y_{2,1} & y_{2,2} & \cdots & y_{2,K} \\ \cdots & \cdots & \cdots & \cdots \\ y_{L,1} & y_{L,2} & \cdots & y_{L,K} \end{bmatrix},$$

$$Z = X \otimes Y = \begin{bmatrix} x_{1,1}y_{1,1} & \cdots & x_{1,1}y_{1,K} & \cdots & x_{1,M}y_{1,1} & \cdots & x_{1,M}y_{1,K} \\ \vdots & \ddots & \vdots & \cdots & \vdots & \ddots & \vdots \\ x_{1,1}y_{L,1} & \cdots & x_{1,1}y_{L,K} & \cdots & x_{1,M}y_{L,1} & \cdots & x_{1,M}y_{L,K} \\ \cdots & \cdots & \cdots & \cdots & \cdots & \cdots & \cdots \\ \cdots & \cdots & \cdots & \cdots & \cdots & \cdots & \cdots \\ x_{N,1}y_{1,1} & \cdots & x_{N,1}y_{1,K} & \cdots & x_{N,M}y_{1,1} & \cdots & x_{N,M}y_{1,K} \\ \vdots & \ddots & \vdots & \cdots & \vdots & \ddots & \vdots \\ x_{N,1}y_{L,1} & \cdots & x_{N,1}y_{L,K} & \cdots & x_{N,M}y_{L,1} & \cdots & x_{N,M}y_{L,K} \end{bmatrix}$$

We first extend the states of the system  $x$  to  $x_\otimes$ :

$$x_\otimes = [x^T x^{[2]T} \cdots x^{[p]T}]^T \quad (10)$$

where  $x^{[p]}$  denotes the  $p$ -th order Kronecker product of  $x$ . For the rest of this paper, a  $p$ -th order  $x_\otimes$  means the term of the highest order in  $x_\otimes$  is  $x^{[p]}$ . So far, there has been no systematic method reported in literature to determine the order of Carleman approximation. In our proposed method, we simulate the system after performing a Taylor expansion. When selecting the order of Taylor expansion, we make sure the truncation error caused by the simulator can be compensated later by the optimizer. We extend Eq. (9) to a bilinear form:

$$\dot{x}_\otimes = \mathcal{A}x_\otimes + \mathcal{A}_0 + \sum_{j=1}^m (\mathcal{B}_j x_\otimes + \mathcal{B}_{j0})u_j, \quad (11)$$

where the nonlinear dynamic information recorded in Tier One approximation is carried by the following extended matrices:  $\mathcal{A}$ ,  $\mathcal{A}_0$ ,  $\mathcal{B}_j$  and  $\mathcal{B}_{j0}$  are matrices of the form:

$$\mathcal{A} = \begin{bmatrix} A_{1,1} & A_{1,2} & \cdots & A_{1,p} \\ A_{2,0} & A_{2,1} & \cdots & A_{2,p-1} \\ 0 & A_{3,0} & \cdots & A_{3,p-2} \\ \cdots & \cdots & \cdots & \cdots \\ 0 & 0 & \cdots & A_{p,1} \end{bmatrix}, \mathcal{A}_0 = \begin{bmatrix} A_{1,0} \\ 0 \\ 0 \\ \cdots \\ 0 \end{bmatrix},$$

$$\mathcal{B}_j = \begin{bmatrix} B_{j1,1} & B_{j1,2} & \cdots & B_{j1,p} \\ B_{j2,0} & B_{j2,1} & \cdots & B_{j2,p-1} \\ 0 & B_{j3,0} & \cdots & B_{j3,p-2} \\ \cdots & \cdots & \cdots & \cdots \\ 0 & 0 & \cdots & B_{jp,1} \end{bmatrix}, \mathcal{B}_{j0} = \begin{bmatrix} B_{j1,0} \\ 0 \\ 0 \\ \cdots \\ 0 \end{bmatrix},$$

where  $A_{k,i} = \sum_{l=0}^{k-1} I_n^{[l]} \otimes A_i \otimes I_n^{[k-1-l]}$  and  $B_{jk,i} = \sum_{l=0}^{k-1} I_n^{[l]} \otimes B_{ji} \otimes I_n^{[k-1-l]}$ . Arriving at Eq. (11) means we have finished Tier

Two approximation. This extended bilinear formulation carries nonlinear dynamic information of the original system.

There are two important assumptions in our proposed approach: (i) The manipulated inputs are all piecewise constant signals within each sampling time. (ii) Each manipulated input enters or can be reformulated to enter the system linearly. This means the system is or can be reformulated as input affine with respect to all manipulated inputs. Fortunately, these two assumptions are commonly satisfied in practice.

Hence, we are able to perform convolution integral and draw an analytical solution to predict system evolution within each sampling time:

$$x(t)_\otimes = \exp \left[ (\mathcal{A} + \sum_{j=1}^m \mathcal{B}_j u_{j,i})(t - T_{i-1}) \right] x(T_{i-1})_\otimes + \int_{T_{i-1}}^t \exp \left[ (\mathcal{A} + \sum_{j=1}^m \mathcal{B}_j u_{j,i})(t - \tau) \right] d\tau \cdot (\mathcal{A}_0 + \sum_{j=1}^m \mathcal{B}_{j0} u_{j,i}) \quad t \in (T_{i-1}, T_i] \quad (12)$$

$$x(T_i)_\otimes = \exp \left[ (\mathcal{A} + \sum_{j=1}^m \mathcal{B}_j u_{j,i}) \Delta T_i \right] x(T_{i-1})_\otimes + (\mathcal{A} + \sum_{j=1}^m \mathcal{B}_j u_{j,i})^{-1} \left[ (\mathcal{A} + \sum_{j=1}^m \mathcal{B}_j u_{j,i}) \Delta T_i - I \right] \cdot (\mathcal{A}_0 + \sum_{j=1}^m \mathcal{B}_{j0} u_{j,i}) \quad (13)$$

This also enables us to perform analytical sensitivity calculation to serve as the search gradient. Detailed derivations are presented in the next section.

Using analytical solutions to predict future economic performance takes less computational efforts. With the search gradient provided, less iterations are required by the optimizer, which further saves computational efforts. This method leads to complexity in modeling the dynamic process. However, since the modeling part is performed off-line, it is an acceptable trade-off for saving tremendous on-line computational efforts.

### C. Sensitivity-based optimization

The economic cost function  $J_e(x, u)$  or  $J_e(x, u_j)$ ,  $j = 1, \dots, m$  can be approximated with the following form:

$$J_e = \sum_{k=0}^{\infty} \sum_{l=0}^{\infty} \frac{1}{(k+l)!} \frac{\partial^{[k+l]} J_e}{\partial x^k \partial u^l} \Big|_0 x^k u^l \quad (14) \cong J_{e,0} + J_{e,A} x_\otimes + \sum_{j=1}^m J_{e,Bj} u_{j,\otimes} + \sum_{j=1}^m J_{e,Nj} u_{j,\otimes} \otimes x_\otimes$$

where  $J_{e,0}$  is a scalar;  $J_{e,A}$ ,  $J_{e,Bj}$  and  $J_{e,Nj}$  are Jacobian matrices. The last term  $\sum_{j=1}^m J_{e,Nj} u_{j,\otimes} \otimes x_\otimes$  is likely to be useful for a non-quadratic economic cost function.

Either the control actions  $u$  or the control moves  $\Delta u$  can be chosen as the design variables, depending on the knowledge of the reference trajectories of the manipulated inputs.

We define the following notations to be used later:

$$\tilde{\mathcal{A}}_{\mathcal{K}} = \mathcal{A} + \sum_{j=1}^m \mathcal{B}_j u_{j,\mathcal{K}}, \quad (15)$$

$$\mathcal{E}_{\mathcal{K}} = \exp(\tilde{\mathcal{A}}_{\mathcal{K}} \Delta T_{\mathcal{K}}), \quad (16)$$

$$\mathcal{G}uU_{\mathcal{K}} = \tilde{\mathcal{A}}_{\mathcal{K}}^{-1} (\mathcal{E}_{\mathcal{K}} - I), \quad (17)$$

$$\mathcal{F}_{\mathcal{K}} = \sum_{j=1}^m \mathcal{B}_j u_{j,\mathcal{K}} + \mathcal{A}_0. \quad (18)$$

where  $I$  is the identity matrix with the corresponding dimension. When constructing the time integral of the economic cost function  $\int_{T_0}^{T_N} J_e dt$ :

$$\begin{aligned} \int_{T_0}^{T_N} J_e dt &\cong J_{e,0}(T_N - T_0) \\ &+ \sum_{i=1}^N [J_{e,A} + \sum_{j=1}^m J_{e,Nj} u_{j,i} \otimes] \int_{T_{i-1}}^{T_i} x_{\otimes} dt \\ &+ \sum_{i=1}^N \sum_{j=1}^m J_{e,Bj} u_{j,i} \Delta T_i \end{aligned} \quad (19)$$

We incorporate the integral of the extended states  $x_{\otimes}$  over each sampling time:

$$\int_{T_{i-1}}^{T_i} x_{\otimes} dt = \mathcal{G}uU_i x_{\otimes,i-1} + \tilde{\mathcal{A}}_i^{-1} (\mathcal{G}uU_i - \Delta T_i \cdot I) \mathcal{F}_i \quad (20)$$

Hence, we free the optimization from the equality constraint that represents the system dynamics.

$u_{k,\mathcal{K}}$  denotes the  $\mathcal{K}$ -th element in the  $k$ -th design variable vector, which is the value of the  $k$ -th manipulated input during the  $\mathcal{K}$ -th sampling time. The sensitivity of the economic cost function to  $u_{k,\mathcal{K}}$  is:

$$\begin{aligned} \frac{\partial}{\partial u_{k,\mathcal{K}}} \int_{T_0}^{T_N} J_e dt &= [J_{e,A} + \sum_{i=\mathcal{K}}^N \sum_{j=1}^m J_{e,Nj} u_{j,i} \otimes] \times \\ &[\int_{T_{\mathcal{K}-1}}^{T_{\mathcal{K}}} \frac{\partial x_{\otimes}}{\partial u_{k,\mathcal{K}}} dt + \int_{T_{\mathcal{K}}}^{T_{\mathcal{K}+1}} \frac{\partial x_{\otimes}}{\partial u_{k,\mathcal{K}}} dt \frac{\partial x_{\otimes,\mathcal{K}}}{\partial u_{k,\mathcal{K}}} \\ &+ \sum_{i=\mathcal{K}+2}^N \int_{T_{i-1}}^{T_i} \frac{\partial x_{\otimes}}{\partial u_{k,\mathcal{K}}} dt (\prod_{l=\mathcal{K}+1}^{i-1} \frac{\partial x_{\otimes,l}}{\partial x_{\otimes,l-1}}) \frac{\partial x_{\otimes,\mathcal{K}}}{\partial u_{k,\mathcal{K}}}] \\ &+ J_{e,Nk} \partial(u_{k,\mathcal{K}})_{\otimes} \otimes \int_{T_{\mathcal{K}-1}}^{T_{\mathcal{K}}} x_{\otimes} dt + J_{e,Bk} \partial(u_{k,\mathcal{K}})_{\otimes} \Delta T_{\mathcal{K}} \end{aligned} \quad (21)$$

The following derivations are used in the sensitivity calculation:

$$\partial(u_{k,\mathcal{K}})_{\otimes} = [1 \quad 2u_{k,\mathcal{K}} \cdots pu_{k,\mathcal{K}}^{p-1}] \quad (22)$$

$$\frac{\partial x_{\otimes,\mathcal{K}}}{\partial x_{\otimes,\mathcal{K}-1}} = \mathcal{E}_{\mathcal{K}} \quad (23)$$

$$\int_{T_{\mathcal{K}-1}}^{T_{\mathcal{K}}} \frac{\partial x_{\otimes}}{\partial x_{\otimes,\mathcal{K}-1}} dt = \mathcal{G}uU_{\mathcal{K}} \quad (24)$$

$$\begin{aligned} \frac{\partial x_{\otimes,\mathcal{K}}}{\partial u_{k,\mathcal{K}}} &= \frac{\partial \mathcal{E}_{\mathcal{K}}}{\partial u_{k,\mathcal{K}}} x_{\otimes,\mathcal{K}-1} \\ &+ \tilde{\mathcal{A}}_{\mathcal{K}}^{-1} \frac{\partial \mathcal{E}_{\mathcal{K}}}{\partial u_{k,\mathcal{K}}} \mathcal{F}_{\mathcal{K}} + \mathcal{G}uU_{\mathcal{K}} \mathcal{B}_{k0} \\ &- \tilde{\mathcal{A}}_{\mathcal{K}}^{-1} \mathcal{B}_k \mathcal{G}uU_{\mathcal{K}} \mathcal{F}_{\mathcal{K}} \end{aligned} \quad (25)$$

$$\begin{aligned} &\int_{T_{\mathcal{K}-1}}^{T_{\mathcal{K}}} \frac{\partial x_{\otimes}}{\partial u_{k,\mathcal{K}}} dt \\ &= \int_{T_{\mathcal{K}-1}}^{T_{\mathcal{K}}} \frac{\partial \mathcal{E}_{\mathcal{K}}}{\partial u_{k,\mathcal{K}}} dt \cdot x_{\otimes,\mathcal{K}-1} \\ &+ \tilde{\mathcal{A}}_{\mathcal{K}}^{-1} \int_{T_{\mathcal{K}-1}}^{T_{\mathcal{K}}} \frac{\partial \mathcal{E}_{\mathcal{K}}}{\partial u_{k,\mathcal{K}}} dt \mathcal{F}_{\mathcal{K}} \\ &+ \tilde{\mathcal{A}}_{\mathcal{K}}^{-1} [\mathcal{G}uU_{\mathcal{K}} - \Delta T_{\mathcal{K}} \cdot I] \mathcal{B}_{k0} \\ &- \tilde{\mathcal{A}}_{\mathcal{K}}^{-1} \mathcal{B}_k \tilde{\mathcal{A}}_{\mathcal{K}}^{-1} [\mathcal{G}uU_{\mathcal{K}} - \Delta T_{\mathcal{K}} \cdot I] \mathcal{F}_{\mathcal{K}} \end{aligned} \quad (26)$$

$\frac{\partial \mathcal{E}_{\mathcal{K}}}{\partial u_{k,\mathcal{K}}}$  and  $\int_{T_{\mathcal{K}-1}}^{T_{\mathcal{K}}} \frac{\partial \mathcal{E}_{\mathcal{K}}}{\partial u_{k,\mathcal{K}}} dt$  can both be computed analytically:

$$\frac{\partial \mathcal{E}_{\mathcal{K}}}{\partial u_{k,\mathcal{K}}} = \sum_{l=1}^{\infty} \frac{(\Delta T_{\mathcal{K}})^l}{l!} \sum_{\lambda=1}^l \tilde{\mathcal{A}}_{\mathcal{K}}^{\lambda-1} \mathcal{B}_k \tilde{\mathcal{A}}_{\mathcal{K}}^{l-\lambda} \quad (27)$$

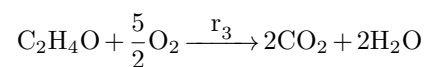
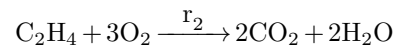
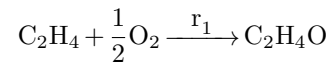
$$\int_{T_{\mathcal{K}-1}}^{T_{\mathcal{K}}} \frac{\partial \mathcal{E}_{\mathcal{K}}}{\partial u_{k,\mathcal{K}}} dt = \sum_{l=1}^{\infty} \frac{(\Delta T_{\mathcal{K}})^{l+1}}{(l+1)!} \sum_{\lambda=1}^l \tilde{\mathcal{A}}_{\mathcal{K}}^{\lambda-1} \mathcal{B}_k \tilde{\mathcal{A}}_{\mathcal{K}}^{l-\lambda} \quad (28)$$

During the optimization, we discretize the system in time by performing convolution integral within each sampling time. We make sure the system behavior satisfies the bounds on the states, the bounds on the manipulated inputs, and the equality/ inequality constraints  $f^c(x, u) \leq 0$  at the end of each sampling time.

### III. APPLICATION AND DISCUSSION

In this section, we demonstrate the proposed Carleman EMPC approach is applicable and computationally efficient by comparing it with the numerical EMPC approach that is the standard method.

As an application example, we consider a CSTR where ethylene is oxidized by air in a catalytic environment [21]. Figure 1 presents a diagram of this reactor. The product is ethylene oxide ( $C_2H_4O$ ). This CSTR is non-isothermal, so a coolant jacket is used to remove heat. The chemical reactions are:



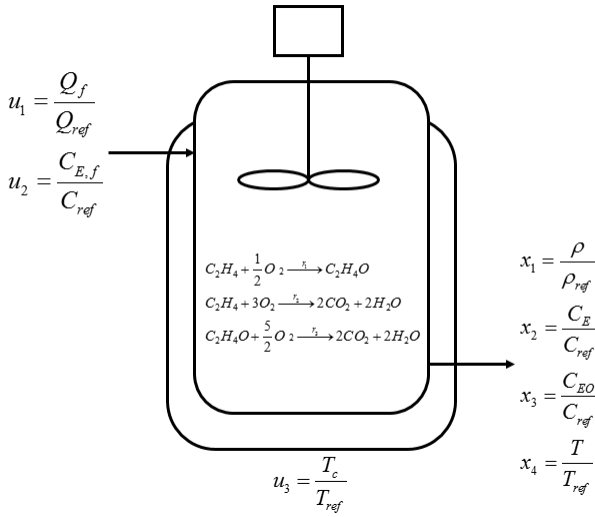


Fig. 1. Diagram of the catalytic ethylene-oxide reactor

where  $r_i, i = 1, 2, 3$  are the reaction rates expressed by

$$\begin{aligned} r_1 &= k_1 \exp\left(\frac{-E_1}{RT}\right) P_E^{\frac{1}{2}} \\ r_2 &= k_2 \exp\left(\frac{-E_2}{RT}\right) P_E^{\frac{1}{4}} \\ r_3 &= k_3 \exp\left(\frac{-E_3}{RT}\right) P_{EO}^{\frac{1}{2}} \end{aligned}$$

$k_i$  and  $E_i, i = 1, 2, 3$  are the reaction rate constant and activation energy, respectively.  $R$  is the ideal gas constant.  $T$  is the temperature.  $P_E$  and  $P_{EO}$  denote the partial pressures of ethylene (E) and ethylene-oxide (EO), respectively. Under the assumption of ideal gas, the concentrations of E and EO can be written as:

$$C_E = \frac{P_E}{RT}, \quad C_{EO} = \frac{P_{EO}}{RT}$$

The states and the manipulated inputs of the system are all normalized and become unit-less:

$$x_1 = \frac{\rho}{\rho_{ref}}, \quad x_2 = \frac{C_E}{C_{ref}}, \quad x_3 = \frac{C_{EO}}{C_{ref}}, \quad x_4 = \frac{T}{T_{ref}}$$

$x_1$  is the normalized vapor density in the reactor.  $x_2$  and  $x_3$  are the concentrations of E and EO in the reactor.  $x_4$  is the normalized reactor temperature.

$$u_1 = \frac{Q_f}{Q_{ref}}, \quad u_2 = \frac{C_{E,f}}{C_{ref}}, \quad u_3 = \frac{T_c}{T_{ref}}$$

$u_1$  is the normalized feeding flow rate.  $u_2$  is the normalized feeding concentration of ethylene.  $u_3$  is the normalized coolant temperature. The dynamic process is described with four ODEs:

$$\begin{aligned} \dot{x}_1 &= u_1(1 - x_1 x_4) \\ \dot{x}_2 &= u_1(u_2 - x_2 x_4) - A_1 \exp\left(\frac{\gamma_1}{x_4}\right)(x_2 x_4)^{\frac{1}{2}} - A_2 \exp\left(\frac{\gamma_2}{x_4}\right)(x_2 x_4)^{\frac{1}{4}} \\ \dot{x}_3 &= -u_1 x_3 x_4 + A_1 \exp\left(\frac{\gamma_1}{x_4}\right)(x_2 x_4)^{\frac{1}{2}} - A_3 \exp\left(\frac{\gamma_3}{x_4}\right)(x_3 x_4)^{\frac{1}{2}} \\ \dot{x}_4 &= \frac{u_1}{x_1}(1 - x_4) + \frac{B_1}{x_1} \exp\left(\frac{\gamma_1}{x_4}\right)(x_2 x_4)^{\frac{1}{2}} + \frac{B_2}{x_1} \exp\left(\frac{\gamma_2}{x_4}\right)(x_2 x_4)^{\frac{1}{4}} \\ &\quad + \frac{B_3}{x_1} \exp\left(\frac{\gamma_3}{x_4}\right)(x_3 x_4)^{\frac{1}{2}} - \frac{B_4}{x_1}(x_4 - u_3) \end{aligned}$$

The parameters are listed in Table I, referring to [22] and [23]. We also refer to [24] to decide our EMPC parameters.

In order to apply the proposed Carleman EMPC method, we define  $u_2^* = u_1 u_2$ , which is the normalized amount of E in the reactor feed, and replace  $u_1 u_2$  with it. Hence, all our manipulated inputs  $u^T = [u_1, u_2^*, u_3]$  are entering the system linearly. We choose an asymptotically stable steady-state  $x_s^T = [0.9980, 0.4235, 0.0320, 1.0020]$  and the corresponding steady-state input  $u_s^T = [0.35, 0.175, 1.0]$  as the nominal point to perform Carleman approximation.

The economic performance of the reactor is characterized by the time-averaged yield of EO:

$$Y(t_f) = \frac{\int_0^{t_f} u_1(\tau) x_3(\tau) x_4(\tau) d\tau}{\int_0^{t_f} u_2^*(\tau) d\tau}$$

which is the amount of EO produced compared with the amount of E fed to the reactor over an operating window  $t_f$ . The amount of E is uniformly provided over each operating window. So our EMPC is subject to the following constraint:

$$\frac{1}{t_f} \int_0^{t_f} u_2^*(\tau) d\tau = 0.175$$

Over each operating window  $t_f = 4.68 \text{ min}$ , the prediction horizon  $N_p = 11$  shrinks at each sampling time,  $N_{p,k} = N_p - k$ , and is reset to  $N_p$  when starting the next operating window. Accumulated constraints are applied to make sure the constraint  $\frac{1}{t_f} \int_0^{t_f} u_2^*(\tau) d\tau = 0.175$  is strictly satisfied. The system is simulated for 10 operating windows.

We use interior-point method as the search algorithm for both standard EMPC approach and the proposed Carleman EMPC approach with Intel Core i7-3770 CPU at 3.40GHz. Standard EMPC is carried out with numerical simulation via Matlab ode45, since the system under investigation has nonlinear dynamics.

In our simulation, the system is initialized at  $x_0^T = [0.997, 1.264, 0.209, 1.004]$ . We simulate the system under nominal condition. Standard EMPC generates a time-averaged yield of 9.22% and spends 226.701 s in calculating the optimal control inputs. The proposed Carleman EMPC achieves a time-averaged yield of 8.81% and spends 83.375 s, which cuts down the computational time by 63.2%.

We also simulate the process under system noise. At each sampling time, bounded Gaussian white noise is added to the system, which has zero mean and a range of  $\delta = \pm[0.005, 0.03, 0.01, 0.02]$ . Figure 2 shows the closed loop

Parameter	Value	Parameter	Value
$A_1$	92.80	$B_3$	2170.57
$A_2$	12.66	$B_4$	7.02
$A_3$	2412.71	$\gamma_1$	-8.13
$B_1$	7.32	$\gamma_2$	-7.12
$B_2$	10.39	$\gamma_3$	-11.07

TABLE I

DIMENSIONLESS PARAMETERS OF THE ETHYLENE OXIDATION CSTR

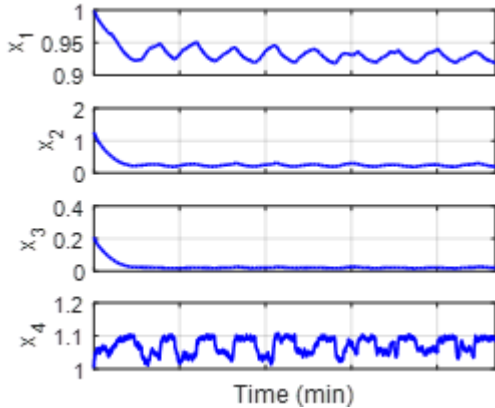


Fig. 2. Standard EMPC: the closed loop performance of the system under system noise

performance of the system under standard EMPC. The time-averaged yield is 9.19% and takes 225.861 s to calculate the economically optimal control policy. In comparison, the simulation under the proposed Carleman EMPC is shown in Figure 3. It generates a time-averaged yield of 8.83% and spends 83.715 s, which saves 62.9% of the computational time.

We test a case where there is a model mismatch between the real system and the parameters we use to design the EMPC controller. The parameter  $\gamma_1$  is assumed to be -10% smaller than the given value in the real system. Figure 4 shows the performance of the closed loop system under standard EMPC scheme. Figure 5 shows the performance under the proposed Carleman EMPC. They are both able to tolerate the model mismatch and generate the same time-averaged yield of 17.6%. The proposed Carleman EMPC spends 125.254 s in computation, which is 36.4% faster than standard EMPC spending 197.014 s.

Therefore, the proposed Carleman EMPC method demonstrates significant computational efficiency. Table II presents a summary of different computational times under different conditions. The difference in the yield probably comes from the approximation of the process and the effect of random noises. In our future work, we will address error prediction methods to compensate for the loss in approximation.

#### IV. CONCLUSIONS

In this paper, we proposed an approach based on Carleman approximation to increase the computational efficiency of EMPC. Our approach readily worked with non-tracking and

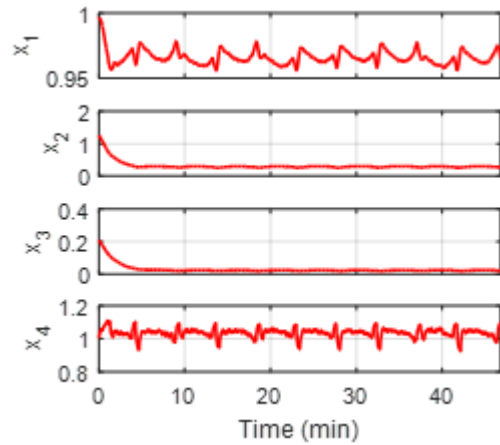


Fig. 3. The proposed Carleman EMPC: the closed loop performance of the system under system noise

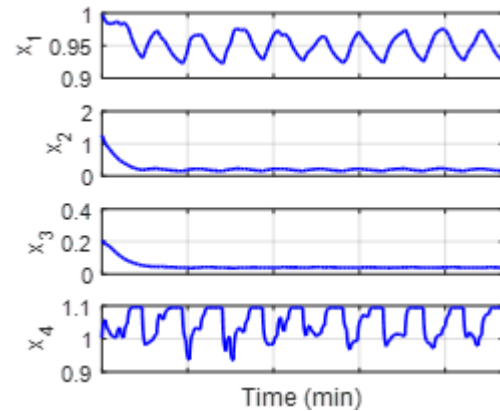


Fig. 4. Standard EMPC: the closed loop performance of the system under model mismatch

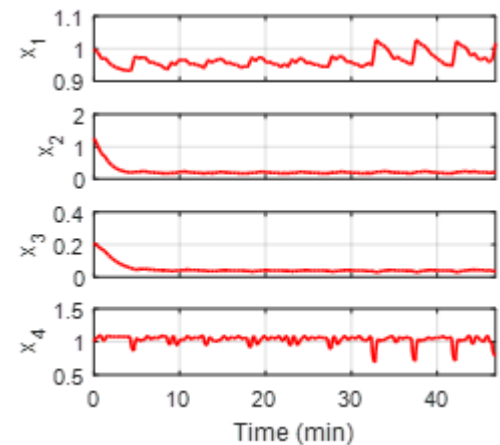


Fig. 5. The proposed Carleman EMPC: the closed loop performance of the system under model mismatch

Condition	Standard EMPC	Carleman EMPC
<i>Nominal</i>	226.701 s	83.375 s
<i>Under system noise</i>	225.861 s	83.715 s
<i>Under model mismatch</i>	197.014 s	125.254 s

TABLE II

COMPARISON OF COMPUTATIONAL TIME: STANDARD EMPC VS THE PROPOSED CARLEMAN EMPC

non-quadratic stage costs of EMPC. We predicted future states and economic performances of the system with fast analytical calculations. We also provided the sensitivity of the economic performance to the manipulated inputs as the search gradient to accelerate optimization. A CSTR producing ethylene-oxide was studied as an application example. We established a non-tracking, cyclic operation. The computational effort was significantly reduced with the proposed Carleman EMPC method.

In our future work, we intend to minimize the loss caused by approximation of the original system. We will also improve our algorithms so they can be applied to more complex systems where the manipulated inputs may not necessarily enter the system in a linear way. In addition, we will apply our proposed method to large-scale EMPC problems to relieve them from heavy computational burden.

## REFERENCES

[1] A. Ferramosca, J. B. Rawlings, D. Limon, and E. F. Camacho, "Economic MPC for a changing economic criterion," *Proc. IEEE Conf. Decis. Control*, pp. 6131-6136, 2010.

[2] R. Amrit, J. B. Rawlings, and L. T. Biegler, "Optimizing process economics online using model predictive control," *Comput. Chem. Eng.*, vol. 58, pp. 334-343, Nov. 2013.

[3] M. Ellis and P. D. Christofides, "Integrating dynamic economic optimization and model predictive control for optimal operation of nonlinear process systems," *Control Eng. Pract.*, vol. 22, pp. 242-251, Jan. 2014.

[4] M. Ellis, H. Durand, and P. D. Christofides, "A tutorial review of economic model predictive control methods," *J. Process Control*, vol. 24, no. 8, pp. 1156-1178, 2014.

[5] M. Diehl, R. Amrit, and J. B. Rawlings, "A Lyapunov Function for Economic Optimizing Model Predictive Control," *IEEE Trans. Automat. Contr.*, vol. 56, no. 3, pp. 703-707, 2011.

[6] M. Heidarinejad, J. Liu, and P. D. Christofides, "Economic model predictive control of switched nonlinear systems," *Syst. Control Lett.*, vol. 62, no. 1, pp. 77-84, Jan. 2013.

[7] A. Armaou and A. Ataei, "Piece-wise constant predictive feedback control of nonlinear systems," *J. Process Control*, vol. 24, no. 4, pp. 326-335, Apr. 2014.

[8] Y. Fang and A. Armaou, "Nonlinear Model Predictive Control Using a Bilinear Carleman linearization-based Formulation for Chemical Processes," *Am. Control Conf. (ACC)*, 2015, no. 1, pp. 5629-5634, 2015.

[9] Y. Fang and A. Armaou, "Carleman approximation based quasi-analytic model predictive control for nonlinear systems," *AICHE J.*, vol. 62, no. 11, pp. 3915-3929, Nov. 2016.

[10] Y. Fang and A. Armaou, "A Formulation of Advanced-step Bilinear Carleman Approximation-based Nonlinear Model Predictive Control," *Proc. 55th IEEE Conf. Decis. Control*, pp. 4027-4032, 2016.

[11] N. Hashemian and A. Armaou, "Fast Moving Horizon Estimation of Nonlinear Processes Via Carleman Linearization," *Am. Control Conf. (ACC)*, 2015, no. 1, pp. 3379-3385, 2015.

[12] N. Hashemian and A. Armaou, "Simulation, Model-Reduction, and State Estimation of a Two-Component Coagulation Process," *AICHE J.*, vol. 62, no. 5, pp. 1557-1567, 2016.

[13] V. Zavala and L. Biegler, "Nonlinear programming strategies for state estimation and model predictive control," in *Nonlinear model predictive control, vol. 384 of Lecture Notes in Control and Information Sciences*, L. Magni, D. Raimondo, and F. Allgower, Eds. Berlin Heidelberg: Springer, 2009, pp. 419-432.

[14] V. Dua and E. Pistikopoulos, "Algorithms for the solution of multiparametric mixed-integer nonlinear optimization problems," *Ind. Eng. Chem. Res.*, vol. 38, pp. 3976-3987, 1999.

[15] V. Dua, N. A. Bozinis, and E. N. Pistikopoulos, "A multiparametric programming approach for mixed-integer quadratic engineering problems," *Comput. Chem. Eng.*, vol. 26, no. 4-5, pp. 715-733, 2002.

[16] J. Liu, G. Li, and H. K. Fathy, "Efficient Lithium-Ion Battery Model Predictive Control Using Differential Flatness-Based Pseudospectral Methods," in *Proceedings of the ASME 2015 Dynamic Systems and Control Conference*, 2015, p. V001T13A005.

[17] J. Liu, G. Li, and H. K. Fathy, "A Computationally Efficient Approach for Optimizing Lithium-Ion Battery Charging," *J. Dyn. Syst. Meas. Control*, vol. 138, no. 2, pp. 21009-1-210098, 2015.

[18] J. Liu, G. Li, and H. K. Fathy, "An Extended Differential Flatness Approach for the Health-Conscious Nonlinear Model Predictive Control of Lithium-Ion Batteries," *IEEE Trans. Control Syst. Technol.*, pp. 1-8, 2016.

[19] V. S. Vassiliadis, R. W. H. Sargent, and C. C. Pantelides, "Solution of a Class of Multistage Dynamic Optimization Problems. 1. Problems without Path Constraints," *Ind. Eng. Chem. Res.*, vol. 33, no. 9, pp. 2111-2122, Sep. 1994.

[20] V. S. Vassiliadis, R. W. H. Sargent, and C. C. Pantelides, "Solution of a Class of Multistage Dynamic Optimization Problems. 2. Problems with Path Constraints," *Ind. Eng. Chem. Res.*, vol. 33, no. 9, pp. 2123-2133, Sep. 1994.

[21] F. Alfani and J. J. Carberry, "An Exploratory Kinetic Study of Ethylene Oxidation Over an Unmoderated Supported Silver Catalyst," *La Chim. e L'Industria*, no. 52, pp. 1192-1196, 1970.

[22] F. Özgülşen, R. Adomaitis, and A. Çinar, "A Numerical Method for Determining Optimal Parameter Values in Forced Periodic Operation," *Chem. Eng. Sci.*, vol. 47, no. 3, pp. 605-613, 1992.

[23] F. Özgülşen, S. J. Kendra, and A. Çinar, "Nonlinear Predictive Control of Periodically Forced Chemical Reactors," *AICHE J.*, vol. 39, no. 4, pp. 589-598, 1993.

[24] M. Ellis and P. D. Christofides, "Optimal Time-varying Operation of Nonlinear Process Systems with Economic Model Predictive Control," *Ind. Eng. Chem. Res.*, vol. 53, pp. 4991-5001, 2014.